Alkyne–carbide coupling on WOs_3 cluster framework; synthesis and X-ray structure of $(C_5Me_5)WOs_3(\mu_4\text{-}C)(\mu\text{-}CHCHR)(CO)_{10}$ and $(C_5Me_5)WOs_3[\mu_3\text{-}CCR(CH_2)](CO)_{10}$, $R = CH_2Ph$

Yun Chi [a],*, Cathy Chung [a], Wen-Cheng Tseng [a], Yung-Chia Chou [a], Shie-Ming Peng [b], Gene-Hsiang Lee [b]

[a] *Department of Chemistry, National Tsing Hua University, Hsinchu 30043, Taiwan ROC*
[b] *Department of Chemistry and Instrumentation Center, National Taiwan University, Taipei 10764, Taiwan ROC*

Abstract

The reaction of the carbido cluster complex $(C_5Me_5)WOs_3(\mu_4\text{-}C)(\mu\text{-}H)(CO)_{11}$ (**1**) with 4-ethynyl toluene is investigated. This reaction results in the formation of an alkylidyne compound $(C_5Me_5)WOs_3(\mu_3\text{-}CCHCHTol)(CO)_{11}$ (**2**) with a *trans* CH=CHTol substituent. Moreover, the corresponding reaction of **1** with 3-phenyl-1-propyne affords an alkenyl carbido cluster $(C_5Me_5)WOs_3(\mu_4\text{-}C)(CHCHCH_2Ph)(CO)_{10}$ (**3**) and another alkylidyne compound with formula $(C_5Me_5)WOs_3[\mu_3\text{-}CC(CH_2Ph)(CH_2)](CO)_{10}$ (**4**). The compounds **3** and **4** are characterized spectroscopically in solution and with single crystal X-ray diffraction in the solid state. The possible mechanism leading to their formation is discussed. © 1999 Elsevier Science S.A. All rights reserved.

Keywords: Alkyne–carbide coupling; WOs_3 cluster framework

1. Introduction

The chemistry of carbido cluster complexes has developed in recent years to constitute a distinct research domain [1]. The majority of the research is focused on the ligand substitution reaction and cluster building reaction [2], in which the carbido atom serves as the supporting group to hold up the surrounding metal atoms, while another less investigated subject involves studying the reactivity of the carbido ligand itself, namely the C–C and C–H bond coupling reaction in the framework of the metal cluster compounds [1a]. The latter is particularly valuable because it represents the key pathway for the conversion of carbides to large hydrocarbon fragments on catalytic metal surfaces [3].

However, the aspect of the C–C and C–H bond coupling reaction of carbide has never been actively perused because the synthetic chemistry leading to the cluster complexes with an exposed carbide is still in an emerging state. On the other hand, when the target molecule can be made in good yield from easily accessible starting materials, systematic investigations of the corresponding reaction with organic molecules have been extensively examined. For example, Bradley [4] and Shriver [5] illustrated that the carbide in the anionic Fe_4 system could react with methanol, alkylation reagents or acids, resulting in the formation of various substituted alkylidyne ligands. In the related neutral Ru_4 complex, Lewis and Johnson reported on the thermally induced, direct coupling of diphenylacetylene with the carbide [6]. Consequently, there should have considerable merit in seeking new examples for such reactions and developing the reactivity of the carbido cluster compounds.

* Corresponding author. Fax: +886-3-572-0864; e-mail: ychi@faculty.nthu.edu.tw.

In pursuing this type of research, the authors have reported on a reversible coupling reaction between carbide and alkylidyne on a pentametallic cluster framework [7], a heretofore unidentified reaction pattern, but which has been extensively discussed according to the conformity between ligated acetylides and carbide–alkylidynes [8]. In this article, the authors report on a related carbide and alkyne coupling involving the carbido cluster $(C_5Me_5)WOs_3(\mu_4\text{-}C)(\mu\text{-}H)(CO)_{11}$ (**1**) with terminal alkynes, 4-ethynyl toluene or 3-phenyl-1-propyne. Interestingly, three products are produced in modest yields by hydride migration to the alkyne in one case, and coupling of the resulting alkenyl fragment with the carbide in the others. The obtained result is in contrast to that of the coupling reaction of **1** with an electron deficient alkyne discussed earlier [9], in which the key reaction step involves the hydride migration to the carbide, highlighting a difference between these seemingly analogous alkyne coupling reactions.

2. Experimental details

2.1. General information and materials

IR spectra were recorded on a Perkin-Elmer 2000 FT-IR spectrometer. ^{1}H- and ^{13}C-NMR spectra were recorded on a Bruker AM-400 (400.13 MHz) or a Bruker AMX-300 (300.6 MHz) instrument, respectively. Mass spectra were obtained on a JEOL-HX110 instrument operating in fast atom bombardment modes (FAB). All reactions were performed under a nitrogen atmosphere using solvents dried with an appropriate reagent. Elemental analyses were performed at the NSC Regional Instrumentation Center at the National Cheng Kung University, Tainan, Taiwan, ROC.

2.2. Reaction of **1** with 4-ethynyl toluene

An acetonitrile solution (20 ml) of freshly sublimed Me$_3$NO (18.4 mg, 0.25 mmol) was added dropwise to a mixture of CH$_2$Cl$_2$ (30 ml), acetonitrile (20 ml) and $(C_5Me_5)WOs_3(\mu_4\text{-}C)(\mu\text{-}H)(CO)_{11}$ (**1**, 200 mg, 0.17 mmol). The addition of Me$_3$NO caused the color of the solution to change from light yellow to orange. Two hours later, the solvents were removed in vacuo and the mixture was redissolved in 50 ml of toluene. 4-Ethynyl toluene (0.84 μl, 0.68 mmol) was added and the resulting solution was heated to reflux for 5 min. The reaction mixture was then concentrated and separated by thin layer chromatography. Development with a 1:2 mixture of CH$_2$Cl$_2$:hexane produced two major bands, which were extracted from silica gel to yield 63 mg of red $(C_5Me_5)WOs_3(\mu_3\text{-}CCHCHTol)(CO)_{11}$ (**2**, 0.047 mmol, 29%) and a second cluster product that contains three 4-ethynyl toluene units, as revealed by FAB MS analysis.

2.2.1. Spectral data for **2**

MS FAB (^{184}W, ^{192}Os): m/z 1332 (M$^+$). IR (C$_6$H$_{12}$): ν(CO), 2076 (s), 2037 (vs), 2027 (vs), 2005 (m), 1993 (w), 1982 (w), 1974 (w), 1967 (w), 1952 (br), 1825 (br, vw) cm^{-1}. ^{1}H-NMR (400 MHz, CDCl$_3$, 293 K): δ 7.95 (d, 1H, J_{HH} = 15 Hz), 7.54 (d, 2H, J_{HH} = 7.9 Hz), 7.22 (d, 1H, J_{HH} = 15 Hz), 7.19 (d, 2H, J_{HH} = 7.9 Hz), 2.31 (s, 3H), 2.09 (s, 15H). ^{13}C-NMR (75 MHz, CDCl$_3$, 294 K): δ 262.8 (J_{WC} = 65 Hz), 224.8 (br, 1CO), 207.1 (br, 1CO), 181.6 (br, 6CO), 179.3 (br, 3CO), 158.1 (CH), 138.0 (i-C$_6$H$_5$), 134.4 (p-C$_6$H$_5$), 131.6 (CH), 130.0 (o-C$_6$H$_5$, 2C), 126.4 (m-C$_6$H$_5$, 2C), 104.3 (C$_5$Me$_5$), 21.5 (CH$_3$), 10.7 (C$_5$Me$_5$). Elem. Anal. for C$_{31}$H$_{24}$O$_{11}$Os$_3$W. Found: C, 28.07; H, 1.79. Calc.: C, 28.06; H, 1.82.

2.3. Reaction of **1** with 3-phenyl-1-propyne

An acetonitrile solution (20 ml) of freshly sublimed Me$_3$NO (43.7 mg, 0.58 mmol) was added dropwise to a mixture of CH$_2$Cl$_2$ (50 ml), acetonitrile (20 ml) and $(C_5Me_5)WOs_3(\mu_4\text{-}C)(\mu\text{-}H)(CO)_{11}$ (**1**, 500 mg, 0.411 mmol). The addition of Me$_3$NO caused the color of solution to change from light yellow to orange. Two hours later the solvents were removed in vacuo and the mixture was redissolved in 80 ml of toluene. 3-Phenyl-1-propyne (0.52 ml, 4.17 mmol) was added and the resulting solution was heated to reflux for 10 min. The reaction mixture was then concentrated and separated by thin layer chromatography. Development with a 1:4 mixture of CH$_2$Cl$_2$:hexane produced two bands, which were extracted from silica gel to yield 200 mg of orange $(C_5Me_5)WOs_3(\mu_4\text{-}C)(CHCHCH_2Ph)(CO)_{10}$ (**3**, 0.154 mmol, 37%) and 79 mg of brown $(C_5Me_5)WOs_3[\mu_3\text{-}CC(CH_2Ph)(CH_2)](CO)_{10}$ (**4**, 0.061 mmol, 15%). Single crystals suitable for X-ray diffraction studies were obtained from a mixture of CH$_2$Cl$_2$ and methanol at r.t.

2.3.1. Spectral data for **3**

MS FAB (^{184}W, ^{192}Os): m/z 1304 (M$^+$). IR (C$_6$H$_{12}$): ν(CO), 2077 (s), 2040 (vs), 2023 (s), 2004 (s), 1981 (s), 1969 (w), 1951 (w), 1888 (w) cm^{-1}. ^{1}H-NMR (600 MHz, CD$_2$Cl$_2$, 293 K): δ 7.38 ∼ 7.32 (m, 5H), 7.24 (t, 1H, J_{HH} = 6.7 Hz), 3.14 ∼ 3.07 (m, 2H), 2.19 (dd, 1H, J_{HH} = 10.5 and 13.2 Hz), 2.06 (s, 15H). ^{13}C-NMR (100 MHz, CDCl$_3$, 293 K): δ 347.3 (J_{WC} = 108 Hz), 216.6 (J_{WC} = 160 Hz), 184.8 (br), 182.3, 179.2 (br), 178.5, 177.4 (br, 2C), 172.1 (br), 169.9 (2C), 141.5 (i-C$_6$H$_5$), 128.7 (o-C$_6$H$_5$, 2C), 128.0 (m-C$_6$H$_5$, 2C), 126.4 (p-C$_6$H$_5$), 122.2 (CH, J_{WC} = 43 Hz), 104.9 (C$_5$Me$_5$), 71.5 (CH), 44.4 (CH$_2$), 11.2 (C$_5$Me$_5$). Elem. Anal. for C$_{30}$H$_{24}$O$_{11}$Os$_3$W. Found: C, 28.20; H, 2.00. Calc.: C, 27.74; H, 1.86.

2.3.2. Spectral data for **4**

MS FAB (^{184}W, ^{192}Os): m/z 1304 (M$^+$). IR (C$_6$H$_{12}$): ν(CO), 2074 (s), 2037 (vs), 2010 (vs), 1998 (s), 1974 (m),

1965 (w), 1946 (w) cm^{-1}. ^{1}H-NMR (400 MHz, CDCl$_3$, 293 K): δ 7.58 (d, 2H, J_{HH} = 7.4 Hz), 7.46 (t, 2H, J_{HH} = 7.4 Hz), 7.36 (t, 1H, J_{HH} = 7.4 Hz), 4.07 (d, 1H, J_{HH} = 13.1 Hz), 3.83 (d, 1H, J_{HH} = 13.1 Hz), 3.71 (s, 1H), 2.12 (s, 1H), 1.73 (s, 15H). ^{13}C-NMR (100 MHz, CDCl$_3$, 293 K): δ 290.8 (J_{WC} = 102 Hz), 220.9 (J_{WC} = 168 Hz), 218.1 (J_{WC} = 156 Hz), 184.4, 183.7, 180.5 (3C), 178.2 (3C), 141.7 (i-C$_6$H$_5$), 129.3 (o-C$_6$H$_5$, 2C), 129.1 (m-C$_6$H$_5$, 2C), 127.4 (p-C$_6$H$_5$), 118.6, 103.5 (C$_5$Me$_5$), 54.1 (CH$_2$), 22.3 (CH$_2$), 10.2 (C$_5$Me$_5$). Elem. Anal. for C$_{30}$H$_{24}$O$_{11}$Os$_3$W. Found: C, 28.10; H, 1.95. Calc.: C, 27.74; H, 1.86.

## 2.4. X-ray crystallography

The X-ray diffraction measurements were carried out on a Nonius CAD-4 diffractometer at r.t. Lattice parameters were determined from 25 randomly selected large angle reflections. Three standard reflections were monitored every 3600 s. No significant change in intensities ($\leq 2\%$) was observed during the course of all data collection. Intensities of the diffraction signals were corrected for Lorentz, polarization and absorption effects (ψ scans). The structure was solved by using the NRCC-SDP-VAX package. All the non-hydrogen atoms had anisotropic temperature factors, while the hydrogen atoms of the organic substituents were placed at the calculated positions with $U_H = U_C + 0.1$. The crystallographic refinement parameters of complexes **3** and **4** are given in Table 1, while their atomic co-ordinates are presented in Tables 2 and 3, respectively. The completed listings of bond distances and angles, tables of anisotropic thermal parameters, and tables of the observed and calculated structural factors are available from the corresponding author.

3. Results and discussion

When the carbido cluster complex (C$_5$Me$_5$)WOs$_3$(μ_4-C)(μ-H)(CO)$_{11}$ (**1**) was first treated with excess of anhydrous Me$_3$NO in a mixed solution of CH$_2$Cl$_2$ and acetonitrile, treatment of this Me$_3$NO-activated compound with 4-ethynyl toluene in refluxing toluene solution produced a red alkylidyne complex (C$_5$Me$_5$)WOs$_3$(μ_3-CCHCHTol)(CO)$_{11}$ (**2**) in low yield (Scheme 1). This compound was fully identified by its spectroscopic data. The FAB MS analysis confirms the formula of C$_{31}$H$_{24}$O$_{11}$Os$_3$W, which is formally produced by the addition of one 4-ethynyl toluene molecule. The IR spectrum in solution shows a CO stretching pattern similar to that of the structurally characterized alkylidyne compounds LWOs$_3$(μ_3-CR)(CO)$_{11}$, L = Cp and C$_5$Me$_5$, R = n-C$_5$H$_{11}$, Tol and H (see Chart 1) [10], providing the unambiguous supporting evidence for the cluster skeletal arrangement.

(Chart 1)
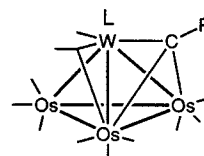
L = Cp, C$_5$Me$_5$; R = H, Me, Ph

The ^{1}H-NMR spectrum shows two doublets at δ 7.95 and 7.54 with coupling constant J_{HH} = 15 Hz, along with the signals expected for the tolyl substituent and the C$_5$Me$_5$ ligand. This observation indicates that the hydride of **1** has migrated to the 4-ethynyl toluene, giving a *trans*-CH=CHTol functional group attached to the alkylidyne ligand, as evidenced by its relatively large $^3J_{HH}$ coupling constant. Accordingly, the ^{13}C-NMR resonance of the alkylidyne α-carbon atom occurs at δ 262.8, while two CH signals appear at the high-field region of δ 158.1 and 131.6. The W-bound CO signals and the Os–CO signals appear as fairly broad signals at r.t. This reflected the enhanced fluxion-

Table 1
X-ray structural data of complexes **3** and **4**[a]

Compound	3	4
Empirical formula	C$_{30}$H$_{24}$O$_{10}$Os$_3$W	C$_{30}$H$_{24}$O$_{10}$Os$_3$W
Formula weight	1298.95	1298.95
Crystal system	Monoclinic	Triclinic
Space group	$P2_1/c$	$P\bar{1}$
a (Å)	20.091(3)	9.503(2)
b (Å)	9.760(1)	10.686(3)
c (Å)	18.031(4)	16.484(5)
α (°)		78.15(3)
β (°)	114.22(2)	77.32(3)
γ (°)		81.08(2)
V (Å^3)	3224(1)	1589.3(7)
Z	4	2
$D_{calc.}$ (g cm^{-3})	2.676	2.712
$F(000)$	2323	1160
2θ (max) (°)	50.0	50.0
h, k, l ranges	$-23 \sim 21$, $0 \sim 11$, $0 \sim 21$	$-10 \sim 11$, $0 \sim 12$, $-18 \sim 19$
Crystal size (mm^3)	$0.10 \times 0.15 \times 0.60$	$0.20 \times 0.30 \times 0.40$
μ(Mo–K$_\alpha$) cm^{-1}	154.82	157.10
Transmission: max, min.	1.000, 0.700	1.000, 0.700
Number of data in refinement	4091 with $I \geq 2\sigma(I)$	4340 with $I \geq 2\sigma(I)$
Number of atoms, parameters	68, 398	67, 398
Weight modifier, g	0.0001	
Maximum Δ/σ ratio	0.002	0.012
R_F; R_w	0.031; 0.30	0.041; 0.047
Goodness-of-fit	1.31	1.34
D-map, max/min (e/Å^3)	1.19/-1.14	2.52/-2.73

[a] Features common to all determinations: Nonius CAD-4 diffractometer, λ(Mo–K$_\alpha$) = 0.7107 Å; minimize function: $\Sigma (w|F_o - F_c|^2)$, weighting scheme: $w^{-1} = \sigma^2(F_o) + g|F_o^2|$; goodness-of-fit = $[\Sigma w|F_o - F_c|^2/(N_o - N_v)]^{1/2}$ (N_o = number of observations; N_v = number of variables).

Table 2
Atomic co-ordinates and isotropic displacement coefficients for complex (**3**); estimated S.D.s refer to the last digit printed

	x	y	z	U_{eq}
Os1	0.88976(3)	0.49877(5)	0.11696(3)	3.554(22)
Os2	0.735761(25)	0.49493(5)	0.036618(24)	3.124(22)
Os3	0.800078(23)	0.69902(4)	0.151274(24)	2.628(20)
W	0.740810(24)	0.46327(4)	0.203071(24)	2.570(20)
C1	0.9768(6)	0.5123(13)	0.2123(7)	4.8(7)
C2	0.9084(8)	0.3216(14)	0.0917(8)	5.9(8)
C3	0.9315(7)	0.5798(14)	0.0443(8)	5.7(8)
C4	0.7258(7)	0.3055(13)	0.0107(7)	5.2(7)
C5	0.7606(7)	0.5527(12)	−0.0489(6)	4.4(7)
C6	0.6363(7)	0.5496(12)	−0.0203(7)	4.6(7)
C7	0.8609(6)	0.7823(11)	0.1040(6)	3.6(6)
C8	0.7239(6)	0.8190(12)	0.0850(7)	4.4(7)
C9	0.8614(6)	0.7847(11)	0.2531(6)	3.8(6)
C10	0.6504(6)	0.3873(11)	0.1209(6)	3.8(6)
C11	0.8154(5)	0.4742(9)	0.1589(6)	2.6(5)
C12	0.7239(6)	0.6744(10)	0.2094(6)	3.1(5)
C13	0.6521(6)	0.6363(11)	0.1640(6)	3.4(5)
C14	0.5927(6)	0.6376(12)	0.1960(6)	4.1(6)
C15	0.5543(6)	0.7753(12)	0.1788(6)	3.8(6)
C16	0.5664(6)	0.8668(12)	0.2386(7)	4.4(7)
C17	0.5330(7)	0.9925(13)	0.2234(10)	6.8(10)
C18	0.4883(8)	1.0311(13)	0.1456(11)	7.7(11)
C19	0.4765(8)	0.9421(17)	0.0855(10)	8.0(10)
C20	0.5085(6)	0.8110(15)	0.1010(7)	5.4(8)
C21	0.7511(6)	0.2526(11)	0.2678(6)	4.0(7)
C22	0.8229(6)	0.3018(12)	0.2926(7)	4.2(6)
C23	0.8281(6)	0.4216(12)	0.3395(6)	4.2(6)
C24	0.7596(6)	0.4453(10)	0.3426(6)	3.0(5)
C25	0.7108(6)	0.3390(10)	0.2972(6)	3.2(5)
C26	0.7241(8)	0.1195(13)	0.2231(8)	6.0 (9)
C27	0.8846(8)	0.2309(15)	0.2839(9)	7.7(10)
C28	0.8953(7)	0.5023(16)	0.3854(8)	6.7(8)
C29	0.7449(7)	0.5497(18)	0.3928(7)	5.0(7)
C30	0.6363(7)	0.3106(12)	0.2909(7)	4.7(7)
O1	1.0252(5)	0.5176(11)	0.2738(5)	7.5(6)
O2	0.9179(6)	0.2101(10)	0.0774(7)	9.4(8)
O3	0.9528(6)	0.6288(11)	0.0020(6)	8.2(7)
O4	0.7191(6)	0.1893(9)	−0.0008(6)	8.4(8)
O5	0.7739(5)	0.5879(10)	−0.1026(5)	6.4(6)
O6	0.5775(5)	0.5834(11)	−0.0563(5)	7.6(6)
O7	0.8906(5)	0.8531(9)	0.0783(5)	5.6(5)
O8	0.6778(5)	0.8873(9)	0.0447(6)	6.6(6)
O9	0.8949(5)	0.8394(10)	0.3120(5)	6.7(6)
O10	0.5940(4)	0.3382(9)	0.0819(5)	5.9(5)

Table 3
Atomic co-ordinates and isotropic displacement coefficients for complex (**4**); eetimated S.D.s refer to the last digit printed

|	x	y	z	U_{eq}
W	0.35374(7)	0.67041(6)	0.30256(4)	2.046(23)
Os1	0.37241(7)	0.89624(6)	0.38112(4)	2.415(25)
Os2	0.13668(7)	0.90251(6)	0.31190(4)	2.288(24)
Os3	0.41027(7)	0.92010(6)	0.20358(4)	2.516(25)
C1	0.5549(19)	0.7050(17)	0.2926(16)	4.4(11)
C2	0.2720(19)	0.6723(15)	0.4236(10)	2.8(7)
C3	0.5606(21)	0.8816(18)	0.4016(13)	3.7(9)
C4	0.2994(21)	0.8750(18)	0.4990(11)	3.5(8)
C5	0.3405(23)	1.0761(17)	0.3622(12)	4.0(10)
C6	0.0249(17)	0.8800(16)	0.4223(10)	2.8(7)
C7	0.0516(21)	1.0722(20)	0.2911(12)	4.2(9)
C8	0.3342(21)	1.0929(19)	0.1620(12)	3.9(9)
C9	0.5850(20)	0.9774(21)	0.2144(13)	4.3(9)
C10	0.491(3)	0.8751(19)	0.0962(13)	4.8(10)
C11	0.2484(15)	0.8010(13)	0.2191(8)	1.8(6)
C12	0.1000(20)	0.8351(17)	0.2021(12)	3.3(8)
C13	−0.0037(20)	0.7927(19)	0.2702(12)	3.7(9)
C14	0.0707(20)	0.9238(19)	0.1204(12)	3.7(8)
C15	0.0589(22)	0.8442(19)	0.0560(12)	4.1(9)
C16	0.172(3)	0.8259(22)	−0.0083(14)	5.2(11)
C17	0.162(3)	0.747(3)	−0.0661(15)	6.4(14)
C18	0.041(4)	0.6916(25)	−0.0560(17)	6.9(16)
C19	−0.073(3)	0.709(3)	0.0088(17)	6.7(15)
C20	−0.0618(25)	0.787(3)	0.0641(15)	5.5(12)
C21	0.2463(21)	0.4794(17)	0.3313(13)	3.7(9)
C22	0.2709(18)	0.5191(16)	0.2426(11)	3.0(7)
C23	0.421(3)	0.5144(19)	0.2144(15)	5.2(11)
C24	0.4905(22)	0.4693(16)	0.2833(12)	3.6(8)
C25	0.3862(22)	0.4491(15)	0.3553(12)	3.4(8)
C26	0.103(3)	0.4522(21)	0.3875(16)	5.3(11)
C27	0.161(3)	0.5293(21)	0.1882(17)	5.6(13)
C28	0.496(4)	0.538(3)	0.1207(16)	8.4(19)
C29	0.647(3)	0.4269(25)	0.2779(23)	7.7(18)
C30	0.415(3)	0.3875(18)	0.4401(16)	5.8(13)
O1	0.6772(14)	0.6997(14)	0.2883(12)	5.8(9)
O2	0.2191(15)	0.6374(12)	0.4936(8)	4.1(7)
O3	0.6763(16)	0.8774(18)	0.4143(11)	6.2(10)
O4	0.2506(18)	0.8646(15)	0.5678(9)	5.5(9)
O5	0.3246(24)	1.1861(13)	0.3479(12)	7.4(11)
O6	−0.0402(15)	0.8639(14)	0.4887(8)	4.5(6)
O7	0.0032(19)	1.1775(14)	0.2741(11)	6.5(8)
O8	0.2951(18)	1.1968 (13)	0.1379(9)	5.6(8)
O9	0.6893(17)	1.0140(18)	0.2186(12)	6.7(9)
O10	0.5402(24)	0.8485(18)	0.0323(10)	7.9(11)

ality of CO ligands due to the rapid terminal-to-bridging CO exchange on the tungsten atom and the tripodal rotation on the osmium metal centers [10d].

The corresponding reaction of **1** with 3-phenyl-1-propyne was then examined, affording two products $(C_5Me_5)WOs_3(\mu_4\text{-}C)(CHCHCH_2Ph)(CO)_{10}$ (**3**) and $(C_5Me_5)WOs_3[\mu_3\text{-}CC(CH_2Ph)(CH_2)](CO)_{10}$ (**4**) in moderate yields (Scheme 2). For these cluster complexes, their FAB MS spectra exhibited a parent ion at m/z 1304, corresponding to the formula $C_{30}H_{24}O_{10}Os_3W$, which is possibly produced by removal of one CO ligand and addition of an alkyne fragment. The ^{1}H-

NMR spectra were then recorded and readily interpreted. Again, no high-field signal was noted, suggesting that the bridging hydride of **1** has migrated
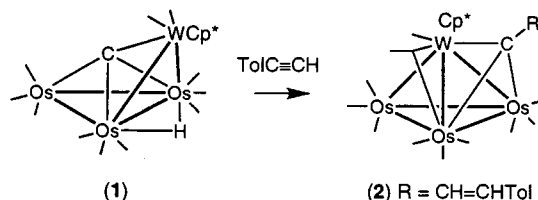
Scheme 1.
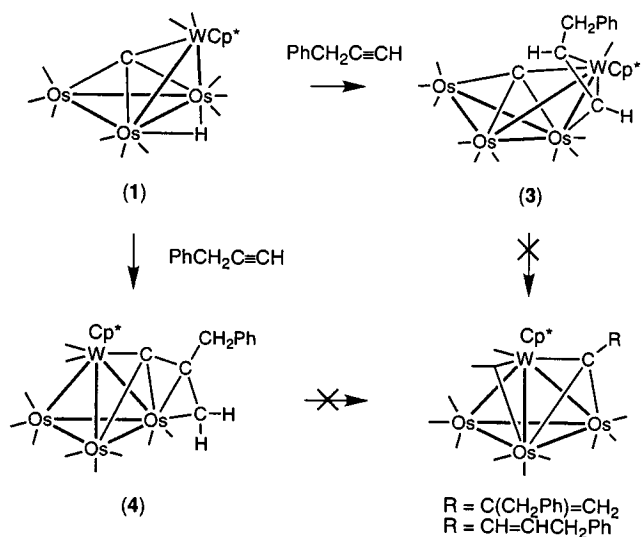
Scheme 2.

to the incoming 3-phenyl-1-propyne. In agreement with this postulation, the formation of two alkenyl resonances at δ 7.24 (t, 1H, $J_{HH} = 6.7$ Hz) and 2.19 (dd, 1H, $J_{HH} = 10.5$ and 13.2 Hz) was observed for complex **3**, along with a complex of multiplets located in the region δ 3.14 ~ 3.07 with an intensity ratio due to two hydrogen atoms, which is attributable to the methylene protons on 3-phenyl-1-propyne. Likewise, for the second complex, **4**, the olefinic and methylene proton resonances are evident by the presence of two doublets at δ 7.58 and 7.46, with a coupling constant $J_{HH} = 7.4$ Hz, and two sharp singlets at δ 3.71 and 2.12, respectively.

On the other hand, the ^{13}C-NMR spectrum of **3** exhibits one down-field carbide signal at δ 347.3 ($J_{WC} = 108$ Hz) and one W–CO ligand at δ 216.6 ($J_{WC} = 160$ Hz); both are indicated by the presence of characteristic J_{WC} coupling, and seven Os–CO signals in the range between δ 184.8 and 169.9. In contrast, the ^{13}C-NMR spectrum of **4** shows no down-field carbido

signal, but gives one relatively high-field signal at δ 290.8 ($J_{WC} = 102$ Hz) that is best assigned to an alkylidyne α-carbon atom [11], together with two W–CO signals at δ 220.9 ($J_{WC} = 168$ Hz) and 218.1 ($J_{WC} = 156$ Hz), and four sharp Os–CO signals at δ 184.4, 183.7, 180.5 and 178.2, with an intensity ratio 1:1:3:3. As these ^{1}H- and ^{13}C-NMR spectroscopic data are still not sufficient to reveal their exact structures, the X-ray diffraction studies were then carried out to reveal the true identity of these products.

The crystals suitable for X-ray diffraction study can be obtained by diffusion of methanol into a CH_2Cl_2 solution at r.t. The ORTEP diagram is depicted in Fig. 1, while the bond distances are summarized in Table 4. The overall structure consists of a typical WOs_3 butterfly skeleton. The W atom is located at a wing-tip position, which is further co-ordinated by a C_5Me_5 and a CO ligand. The remaining nine CO ligands are equally distributed over three osmium atoms. The carbido atom C(10) is bound to all four metal atoms with short M(wing-tip)–C distances (average 1.96(4) Å) and long M(hinge)–C distances (average 2.17(4) Å). This observed bond pattern is typical for the carbido atom in the butterfly environment [12]. For a comparison, a similar skeletal arrangement has been observed in the related tetrametallic carbido clusters CpWRu$_3(\mu_4$-C)(μ-H)(CO)$_{11}$ [13] and CpWOs$_3(\mu_4$-C)(μ-SMe)(CO)$_{11}$ [14] and the closely related carbonyl clusters $(C_5Me_5)MRu_3(\mu_4$-CO)(μ-H)(CO)$_{11}$, M = Mo and W, with a quadruply bridging CO ligand to replace the carbide fragment [15].

In addition, it was observed that the 3-phenyl-1-propyne in **4** has now converted to a *trans*-vinyl fragment CH=CHCH$_2$Ph by placing a hydrogen on the atom C(13). This bridging vinyl group is linked to the atom Os(3) through a σ-interaction and to the W atom via a dative π-interaction, although the observed W–C(12) distance (2.099(10) Å) is slightly shorter than that of the Os(3)–C(12) distance (2.193(10) Å). In fact,

Table 4
Selected bond lengths (Å) and angles (°) of **3** (eetimated S.D. in parentheses)

Bond lengths (Å)

W–Os(2)	2.9773(9)	W–Os(3)	2.9150(7)
Os(1)–Os(2)	2.8275(9)	Os(1)–Os(3)	2.8921(7)
Os(2)–Os(3)	2.7785(7)	W–C(11)	1.968(9)
Os(1)–C(11)	1.945(9)	Os(2)–C(11)	2.137(10)
Os(3)–C(11)	2.212(9)	W–C(12)	2.099(10)
W–C(13)	2.344(10)	Os(3)–C(12)	2.193(10)
C(12)–C(13)	1.39(2)	C(13)–C(14)	1.52(2)

Bond angles (°)

W–C(11)–Os(1)	176.0(5)	Os(2)–C(11)–Os(3)	79.4(3)
W–C(10)–O(10)	169.7(9)	Os–CO	176.5 ~ 179.7(19)

Table 5
Selected bond lengths (Å) and angles (°) of **4** (estimated S.D. in parentheses)

Bond length (Å)

W–Os(1)	3.008(1)	W–Os(2)	2.978(1)
W–Os(3)	2.888(1)	Os(1)–Os(2)	2.717(1)
Os(1)–Os(3)	2.832(1)	Os(2)–Os(3)	2.823(1)
W–C(11)	2.06(1)	Os(2)–C(11)	2.06(1)
Os(3)–C(11)	2.09(1)	Os(2)–C(12)	2.19(2)
Os(2)–C(13)	2.20(2)	C(11)–C(12)	1.48(2)
C(12)–C(13)	1.37(3)	C(12)–C(14)	1.53(3)

Bond angles (°)

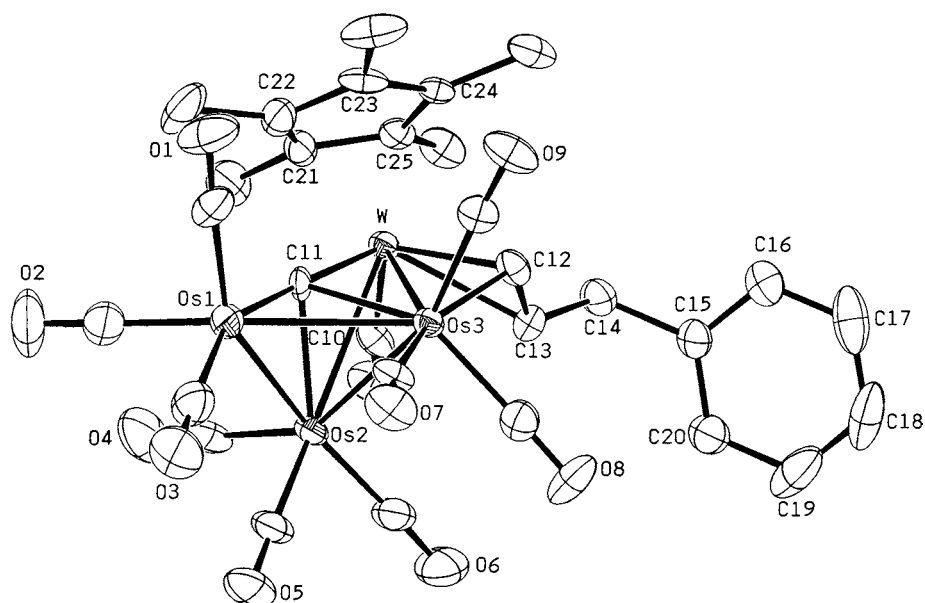|			
W–C(1)–O(1)	167(1)	W–C(2)–O(2)	160(1)
Os–CO	167.1 ~ 178.3(10)		

Fig. 1. Molecular structure and atomic labeling scheme of the complex $(C_5Me_5)WOs_3(\mu_4\text{-}C)(CHCHCH_2Ph)(CO)_{10}$ (**3**) with thermal ellipsoids shown at the 30% probability level.

such a structural feature is common for the cluster compounds bearing an edge-bridging vinyl ligand and is also consistent with the parameters observed in a closely related cluster complex $(C_5Me_5)WOs_3(\mu_4\text{-}C)(\mu\text{-}CHCHOMe)(CO)_{10}$ [7c].

In contrast to that of complex **3**, the cluster core of **4** consists of a tetrahedral geometry composed of a $(C_5Me_5)W(CO)_2$ vertex, together with two $Os(CO)_3$ and one $Os(CO)_2$ units that form a metal triangle at the basal position (Fig. 2). The W–Os distances span the range 2.888(1) ∼ 3.008(1) Å, while the Os–Os distances are slightly shorter with the Os(1)–Os(2) distance 2.717(1) Å being the shortest of whole molecule (see Table 5). This variation of metal–metal distances fall within the expected range for the 60 electron, tetrahedral WOs_3 cluster compound [16]. The alkylidyne α-carbon atom C(11), which is obviously derived from the carbide ligand of **1**, resides on the W–Os(2)–Os(3) metal triangle with three nearly equal metal–carbon distances 2.06(1) ∼ 2.09(1) Å, and is linked to an alkenyl fragment, CH_2=CCH_2Ph substituent. This newly formed alkenyl group, produced by hydride migration to the terminal carbon of 3-phenyl-1-propyne, is further co-ordinated to the unique $Os(CO)_2$ vertex with slightly elongated bond lengths Os(2)–C(12) = 2.19(2) Å and Os(2)–C(13) = 2.20(1) Å. If this secondary olefinic π-interaction is ignored, the overall geometry is analogous to that of the previously discussed alkylidyne complex **2**, for which the cluster skeleton possess a face-bridging alkylidyne ligand and three $Os(CO)_3$ metal vertices at the basal positions.

4. Discussion

As stated above, treatment of **1** with Me_3NO, followed by addition of 4-ethynyl toluene or 3-phenyl-1-propyne leads to the isolation of three stable cluster compounds **2**, **3** and **4** in moderate yields. Attempts to duplicate this coupling reaction by the direct treatment of **1** with the alkyne were unsuccessful, suggesting that the prior addition of Me_3NO is crucial in activating the carbido cluster compound **1**. By analogy to other alkyne coupling reactions using Me_3NO as the initiator [17], the authors believe that the first step is the removal of a CO ligand from an osmium atom, which offers a lower energy pathway for the incoming alkyne molecule to link to the cluster framework. After that, the hydride migration to the alkyne and simultaneous coupling with the carbide would give rise to the formation of vinyl alkylidyne clusters **2** and **4**. If the reaction stopped after the hydride migration to alkyne, formation of the carbido alkenyl complex **3** is envisioned without the accompanied carbide–alkenyl coupling. Interestingly, it is tempting to say that complexes **3** and **4** are related to the alkylidyne complex **2** through two independent hypothetical transformations (Scheme 2) involving the C–C bond formation between carbide and alkenyl ligand or the removal of alkenyl π-bonding, respectively. However, heating of the complexes **3** or **4** at 110°C under CO atmosphere for 30 min led to neither the formation of such alkylidyne complexes nor decomposition. These observations terminate the current attempt to delineate the mechanistical relationship between complexes **2**, **3** and **4**.
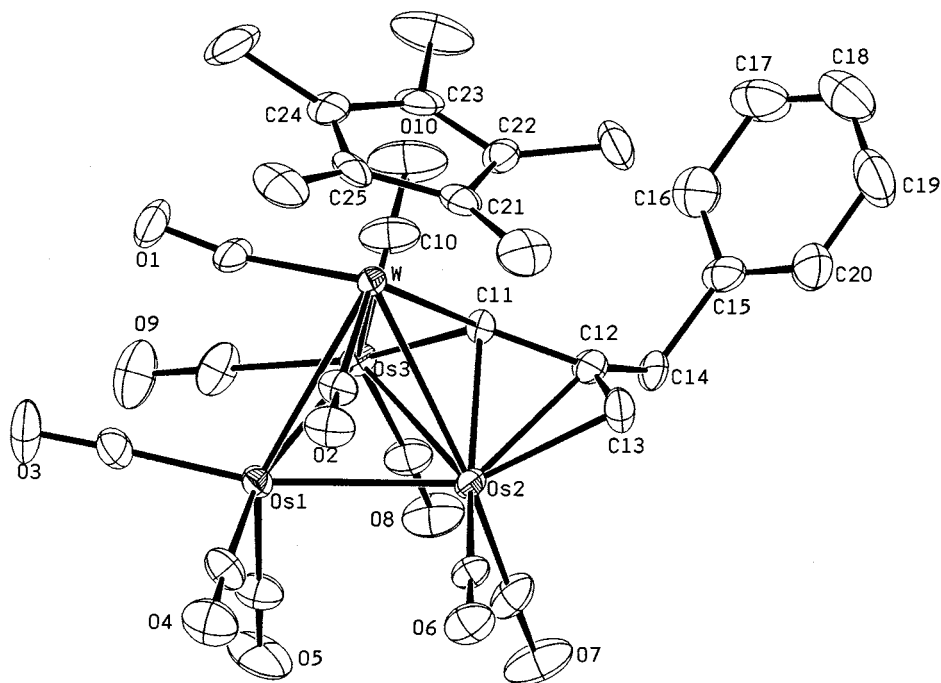
Fig. 2. Molecular structure and atomic labeling scheme of the complex $(C_5Me_5)WOs_3[\mu_3\text{-}CC(CH_2Ph)(CH_2)](CO)_{10}$ (4) with thermal ellipsoids shown at the 30% probability level.

Still, these results are in contrast to those reported in a preceding paper dealing with the coupling of 1 with an electron deficient alkyne, diisopropyl acetylenedicarboxylate (DPAD) [9], in which the authors observed the formation of a dimetallaallyl cluster $(C_5Me_5)WOs_3$ $(CO)_{10}[C_3H(CO_2i\text{-}Pr)_2]$ (5) as the major product, then underwent C–C bond metathesis to afford a second dimetallaallyl cluster (6) with the CH group moved to the central position (Scheme 3). Obviously, the dimetallaallyl fragment in 5 is produced by an independent process involving hydride migration to the carbide and coupling with DPAD. The origin of these differing

behaviors is not known; however, it is possible that the electron deficiency on DPAD would somehow increase the activation barrier for alkyne–hydride coupling. Thus, the reaction proceeded through a pathway characterized by the carbide–hydride coupling to give a methylidyne ligand, followed by methylidyne–alkyne coupling, a process that is well-established in literature [18]. On the other hand, trace amounts of a related vinyl–alkylidyne cluster (7) was observed as a minor product for the reaction of 1 with DPAD in refluxing toluene solution, suggesting that the hydride migration to alkyne was more favorable at the higher reaction temperature. Thus, the chemistry observed in present study provides an unambiguous experimental model for the less accessible route of the coupling between hydride, alkyne and carbide on the WOs_3 tetrametallic cluster framework.

Acknowledgements

References

[1] (a) J.S. Bradley, Adv. Organomet. Chem. 22 (1982) 1. (b) J. Lewis, B.F.G. Johnson, Pure Appl. Chem. 54 (1982) 97. (c) B.F.G. Johnson, J. Lewis, W.J.H. Nelson, J.N. Nicholls, M.D.
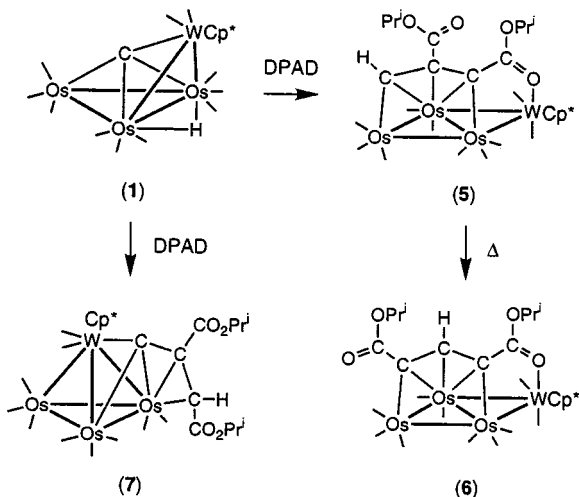
Scheme 3.

Vargas, J. Organomet. Chem. 249 (1983) 255. (d) M.P. Jensen, W. Henderson, D.H. Johnston, M. Sabat, D.F. Shriver, J. Organomet. Chem. 394 (1990) 121. (e) R.D. Adams, W. Wu, Organometallics 12 (1993) 1238. (f) G.B. Karet, R.L. Espe, C.L. Stern, D.F. Shriver, Inorg. Chem. 31 (1992) 2658. (g) T. Chihara, H. Yamazaki, J. Organomet. Chem. 428 (1992) 169. (h) Y. Takahashi, M. Akita, Y. Moro-Oka, Chem. Commun. (1997) 1557.

[2] (a) A.J. Blake, J.L. Haggitt, B.F.G. Johnson, S. Parsons, J. Chem. Soc. Dalton Trans. (1997) 991. (b) G. Freeman, S.L. Ingham, B.F.G. Johnson, M. McPartlin, I.J. Scowen, J. Chem. Soc. Dalton Trans. (1997) 2705. (c) R.D. Adams, W. Wu, J. Cluster Sci. 4 (1993) 245. (d) P.J. Dyson, B.F.G. Johnson, J. Lewis, D. Braga, P. Sabatino, J. Chem. Soc. Chem. Commun. (1993) 301. (e) J.L. Haggitt, B.F.G. Johnson, A.J. Blake, S. Parsons, J. Chem. Soc. Chem. Commun. (1995) 1263. (f) G. Hsu, S.R. Wilson, J.R. Shapley, Organometallics 13 (1994) 4159. (g) T. Chihara, H. Yamazaki, J. Chem. Soc. Dalton Trans. (1995) 1369.

[3] (a) M. Tachikawa, E.L. Muetterties, J. Am. Chem. Soc. 102 (1980) 4541. (b) J.A. Hriljac, P.N. Swepston, D.F. Shriver, Organometallics 4 (1985) 158. (c) P.L. Bogdan, C.P. Horwitz, D.F. Shriver, J. Chem. Soc. Chem. Commun. (1986) 553.

[4] (a) J.S. Bradley, G.B. Ansell, E.W. Hill, J. Am. Chem. Soc. 101 (1979) 7417. (b) J.S. Bradley, E.W. Hill, G.B. Ansell, M.A. Modrick, Organometallics 1 (1982) 1634.

[5] (a) E.M. Holt, K.H. Whitmire, D.F. Shriver, J. Organomet. Chem. 213 (1981) 125. (b) E.M. Holt, K.H. Whitmire, D.F. Shriver, J. Am. Chem. Soc. 104 (1982) 5621. (c) S.D. Wijeyesekera, R. Hoffmann, C.N. Wilker, Organometallics 3 (1984) 962. (d) P.L. Bogdan, C. Woodcock, D.F. Shriver, Organometallics 6 (1987) 1377.

[6] T. Dutton, B.F.G. Johnson, J. Lewis, S.M. Owen, P.R. Raithby, J. Chem. Soc. Chem. Commun. (1988) 1423.

[7] (a) S.-J. Chiang, Y. Chi, P.-C. Su, S.-M. Peng, G.-H. Lee, J. Am. Chem. Soc. 116 (1994) 11 181. (b) Y. Chi, P.-C. Su, S.-M. Peng, G.-H. Lee, Organometallics 14 (1995) 5483. (c) P.-C. Su, Y. Chi, C.-J. Su, S.-M. Peng, G.-H. Lee, Organometallics 16 (1997) 1870.

[8] (a) A.J. Carty, Pure Appl. Chem. 54 (1982) 113. (b) A.J. Carty, N.J. Taylor, E. Sappa, A. Tiripicchio, M.T. Camellini, Organometallics 10 (1991) 1907. (c) P. Blenkiron, N.J. Taylor, A.J. Carty, J. Chem. Soc. Chem. Commun. (1995) 327.

[9] C. Chung, W.-C. Tseng, Y. Chi, S.-M. Peng, G.-H. Lee, Organometallics 17 (1998) 2207.

[10] (a) J. Busetto, M. Green, B. Hessner, J.A.K. Howard, J.C. Jeffery, F.G.A. Stone, J. Chem. Soc. Dalton Trans. (1983) 519. (b) Y. Chi, G.-H. Lee, S.-M. Peng, C.-H. Wu, Organometallics 8 (1989) 1574. (c) J.-H. Gong, C.-C. Chen, Y. Chi, S.-L. Wang, F.-L. Liao, J. Chem. Soc. Dalton Trans. (1993) 1829. (d) J.-H. Gong, D.-K. Hwang, C.-W. Tsay, Y. Chi, S.-M. Peng, G.-H. Lee, Organometallics 13 (1994) 1720.

[11] (a) J. Evans, S.C. McNulty, J. Chem. Soc. Dalton Trans. (1984) 79. (b) J.T. Park, Y. Chi, J.R. Shapley, M.R. Churchill, J.W. Ziller, Organometallics 13 (1994) 813.

[12] (a) S. Harris, J.S. Bradley, Organometallics 3 (1984) 1086. (b) J.A. Hriljac, S. Harris, D.F. Shriver, Inorg. Chem. 27 (1988) 816.

[13] Y. Chi, S.-H. Chuang, B.-F. Chen, S.-M. Peng, G.-H. Lee, J. Chem. Soc. Dalton Trans. (1990) 3033.

[14] J.-H. Gong, C.-W. Tsay, W.-C. Tu, Y. Chi, S.-M. Peng, G.-H. Lee, J. Cluster Sci. 6 (1995) 289.

[15] (a) Y. Chi, F.-J. Wu, B.-J. Liu, C.-C. Wang, S.-L. Wang, J. Chem. Soc. Chem. Commun. (1989) 873. (b) Y. Chi, C.-J. Su, L.J. Farrugia, S.-M. Peng, G.-H. Lee, Organometallics 13 (1994) 4167.

[16] (a) M.R. Churchill, F.J. Hollander, J.R. Shapley, D.S. Foose, J. Chem. Soc. Chem. Commun. (1978) 534. (b) Y. Chi, C.-Y. Cheng, S.-L. Wang, J. Organomet. Chem. 378 (1989) 45.

[17] (a) J.T. Park, J.R. Shapley, C. Bueno, J.W. Ziller, M.R. Churchill, Organometallics 7 (1988) 2307. (b) Y. Chi, G. Huttner, W. Imhof, J. Organomet. Chem. 384 (1990) 93.

[18] (a) M.K. Alami, F. Dahan, R. Mathieu, Organometallics 4 (1985) 2122. (b) L.R. Beanan, J.B. Keister, Organometallics 4 (1985) 1713. (c) M.R. Churchill, J.W. Ziller, J.R. Shapley, W.-Y. Yeh, J. Organomet. Chem. 353 (1988) 103. (d) D. Lentz, H. Michael-Schulz, Inorg. Chem. 29 (1990) 4396. (e) W.-Y. Wong, S. Chan, W.-T. Wong, J. Chem. Soc. Dalton Trans. (1995) 1497.